Collagen and Leather

RESEARCH

Open Access

Injectable dECM-enhanced hyaluronic microgels with spatiotemporal release of cartilage-specific molecules to improve osteoarthritic chondrocyte's function

Siyan Deng[1,2], Hongfu Cao[1,2], Yan Lu[1,2], Wenqing Shi[1,2], Manyu Chen[1,2], Xiaolin Cui[3,4], Jie Liang[1,2,5], Yujiang Fan[1,2*], Qiguang Wang[1,2*] and Xingdong Zhang[1,2]

Abstract

The interior environment of articular cartilage in osteoarthritis (OA) presents substantial hurdles, leading to the malfunction of chondrocytes and the breakdown of collagen II-enriched hyaline cartilage matrix. Despite this, most clinical treatments primarily provide temporary relief from OA discomfort without arresting OA progression. This study aimed to alleviate OA by developing intra-articular injectable dECM-enhanced hyaluronic (HE) microgels. The HE hydrogel was engineered and shaped into uniformly sized microgels using microfluidics and photopolymerization techniques. These microgels provided a spatiotemporal cascade effect, facilitating the rapid release of growth factors and a slower release of ECM macromolecules and proteins. This process assisted in the recovery of OA chondrocytes' function, promoting cell proliferation, matrix synthesis, and cartilage-specific gene expression in vitro. It also effectively aided repair of the collagen II-enriched hyaline cartilage and significantly reduced the severity of OA, as demonstrated by radiological observation, gross appearance, histological/immunohistochemical staining, and analysis in an OA rat model in vivo. Collectively, the HE injectable microgels with spatiotemporal release of cartilage-specific molecules have shown promise as a potential candidate for a cell-free OA therapy approach.

Keywords Osteoarthritis, Decellularized cartilage matrix, Hyaluronic acid, Spatiotemporal release, Intra-articular injection

*Correspondence:
Yujiang Fan
fan_yujiang@scu.edu.cn
Qiguang Wang
wqgwang@126.com
Full list of author information is available at the end of the article

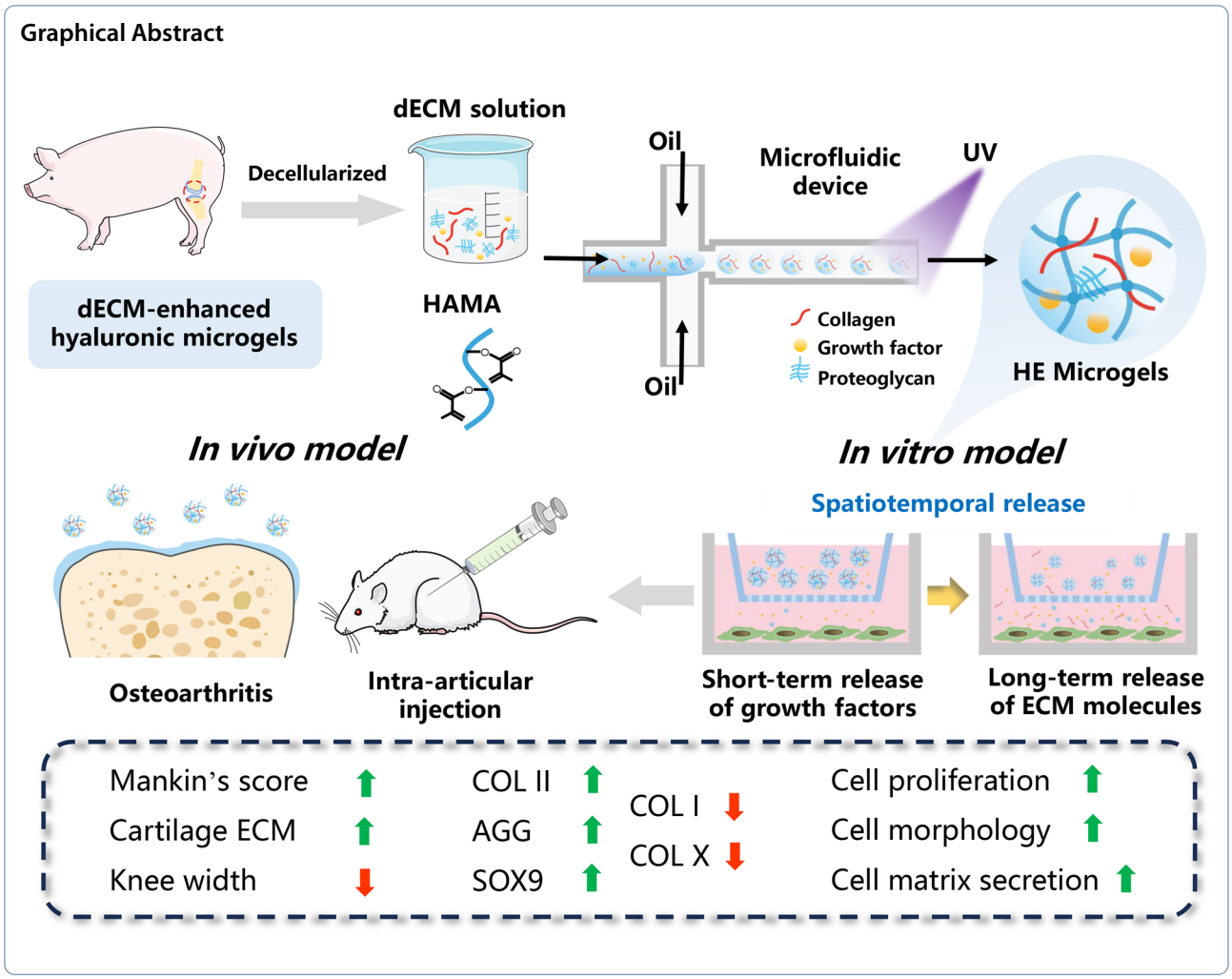

1 Introduction

Osteoarthritis (OA) is a prevalent chronic disease that afflicts hundreds of millions of people worldwide each year [1]. It is characterized by pain, an inflammatory response, joint destabilization, and the loss of collagen II-enriched hyaline cartilage, ultimately affecting the entire joint. Early treatment of OA often involves the use of pharmacological interventions such as non-steroidal anti-inflammatory drugs (NSAIDs), corticosteroids, and analgesics to alleviate pain [2, 3]. However, these treatments frequently fail to halt further deterioration of the joint structure and microenvironment and are associated with adverse effects [4, 5]. Once the disease advances to a severe stage, surgical joint replacement becomes the only viable treatment option. Thus, it is crucial to develop effective intervention programs that target the early stages of OA.

Intra-articular hyaluronic acid (HA) injections have been extensively used in OA treatment, providing effective pain relief and symptomatic therapy [6]. HA, a glycosaminoglycan found abundantly in synovial fluid, plays a crucial role in protecting articular cartilage and promoting cartilage regeneration due to its inherent properties, particularly viscoelasticity [7]. High molecular weight HA, which is often reduced in OA joints, maintains the rheological homeostasis of the synovial fluid and helps dampen shock, lubricate, and nourish joint tissues [8, 9]. Therefore, intra-articular HA injections have been shown to function as viscosupplementation, leading to significant functional improvement in OA joints. However, most HA preparations have a short half-life in the joints due to rapid clearance and swift degradation in vivo by enzymatic or hydrolytic reactions, remaining in the joints for only a few hours to a couple of days [6, 10, 11]. Consequently, achieving effective treatment results often requires multiple injections, which can lead to difficulties in ensuring patient compliance and an increased risk of side effects.

Therefore, it is essential to optimize biomaterials for intra-articular injections to aid in OA treatment.

Injectable hydrogels have been widely investigated for use in OA arthrocentesis due to their slow degradation, enhanced stability, and strong adhesion, which allows for prolonged retention [12, 13]. However, the irregular shape and large size of hydrogels can lead to high and uneven injection forces during injection [14], potentially damaging healthy tissues in the affected area. Compared to block hydrogels, hydrogel microspheres, also known as microgels, with their uniform size and spherical shape, provide improved injectability [15, 16]. Among the various production methods, microfluidics offers significant advantages such as the rapid generation of microgels with precise and consistent sizes [17]. Consequently, HA-based microgels have been extensively studied and have shown to effectively extend the degradation of HA, provide lubrication, and offer biocompatibility. However, within the complex intra-articular joint environment, a single HA component has limited capacity to replace the cartilaginous extracellular matrix and offer multifunctionality.

The extracellular matrix (ECM) serves as a natural structure for cell adhesion, proliferation, migration, and differentiation, in addition to providing biomechanical capabilities. The decellularized ECM (dECM), derived by eliminating cellular components and genetic material from the ECM of human or animal tissues using decellularization techniques, reduces immunogenicity and is a promising biomaterial highly regarded in regenerative tissue engineering applications, such as skin, cornea, and nerve [18, 19]. Cartilage tissue-derived dECM has been demonstrated to provide structural and functional proteins that support cell attachment, growth, and differentiation specific to cartilage tissue [20]. The dECM retains most cartilage-specific matrix macromolecules, including primarily collagen II and proteoglycans, along with less abundant components such as fibulin and elastin. These contribute to the production and maintenance of ECM, enhance chondrocyte morphology and phenotype, ensure cartilage homeostasis, and regulate newborn cartilage tissues through various cytokines, enzymes, and signaling pathways [21–24]. Moreover, it contains numerous growth factors involved in chondrocyte function, including transforming growth factor-β (TGF-β), insulin-like growth factor-1 (IGF-1), bone morphogenetic protein (BMP), fibroblast growth factor (FGF), and epidermal growth factor (EGF) [25]. Members of the TGF-β superfamily play a pivotal role in cartilage development and repair [26, 27]; IGF-1 stimulates the anabolic activity of chondrocytes and inhibits chondrocyte apoptosis [28, 29]; BMPs, particularly BMP-2 and BMP-7, promote chondrogenesis in MSCs and enhance chondrocyte matrix production [30, 31]. In addition to growth factors, Therefore, cartilage-derived dECM, due to its similarity to the natural microenvironment and the bioactivity of cartilage formation, exhibits beneficial effects on tissue morphogenesis, differentiation, homeostasis, and repair.

This study aimed to enhance the HA-based hydrogel formulation, referred to HE, by incorporating a solution derived from cartilage dECM to augment the limited bio-functionality of HA and improve the injectability of dECM. The HE microgels were fabricated using microfluidics and photopolymerization, ensuring their uniform size and mechanical strength for effective lubrication and durability under extensive joint movements. It was hypothesized that the HE microgels facilitate a spatiotemporal cascade effect, with cartilage-specific growth factors being released in the short term to prompt the swift restoration of OA chondrocyte function. Concurrently, the extended release of structural ECM macromolecules and collagens offers a sustained supply of essential components, which are vital for cartilage regeneration and the maintenance of homeostasis as the HE microgels degrade. This combined process was anticipated to produce synergistic and enduring effects across the various stages of OA chondrocyte recovery and cartilage regeneration, including improved viability of OA chondrocytes, enhanced matrix secretion, collagen II synthesis, and the preservation of cellular function and cartilage matrix integrity, potentially offering a therapeutic approach for OA. To validate this hypothesis, the effects of HE microgels on OA chondrocyte proliferation, morphology, and matrix secretion were investigated in vitro. The findings were further corroborated through intra-articular injection in a rat OA model in vivo (Scheme 1).

2 Materials and methods

2.1 Materials

Hyaluronic acid (HA, Mw = 0.94 MDa) was purchased from Florida Biochemistry Limited (Shandong, China). Methacrylic anhydride (MA) was obtained from Chengdu Chemical Xia Reagent Co. Liquid paraffin and Span 80 were purchased from Cologne Chemical (Chengdu, China). 3-[(3-cholamidopropyl) dimethylamino] propanesulfonic acid internal salt (CHAPS) were bought from Sigma-Aldrich (USA). Hyaluronidase, type I collagenase and DNase I were obtained from Solarbio (Beijing, China). α-MEM medium was bought from Servicebio (Wuhan, China). Penicillin–streptomycin and parenzyme were purchased from Hyclone (USA). Fetal bovine serum (FBS, Gibco, KEEL) was obtained from Life Technologies Corporation (USA). Fluorescein diacetate (FDA) and propidium iodide (PI) were bought from Sigma-Aldrich (USA).

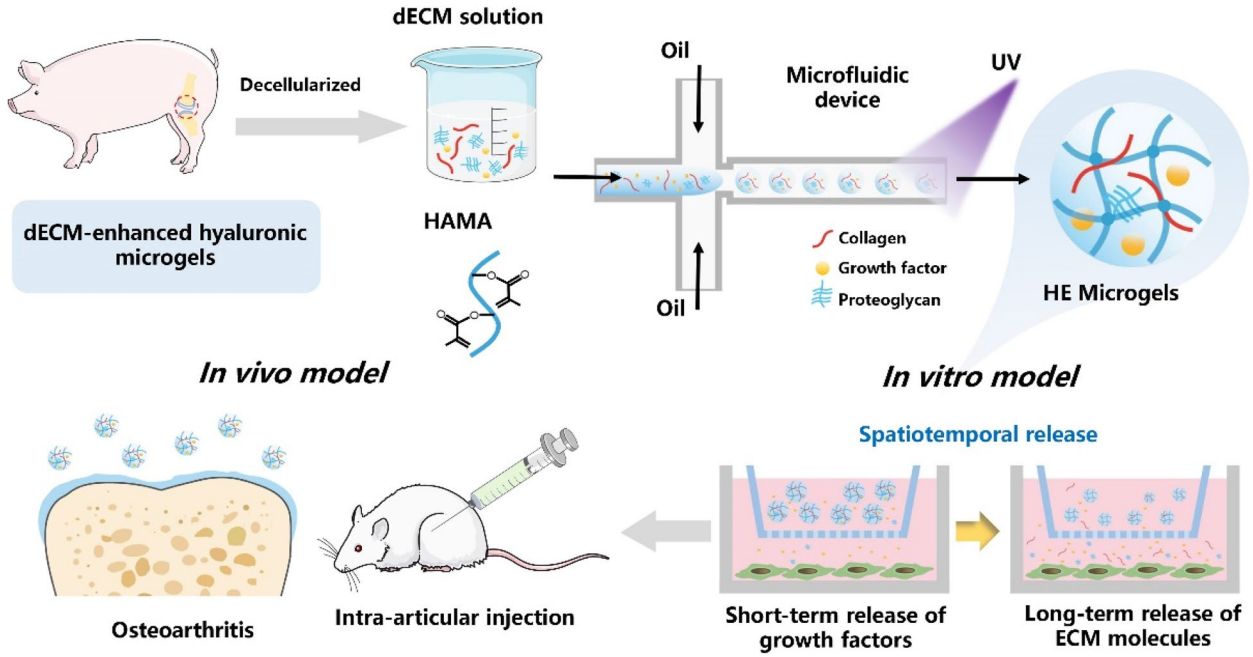

Scheme 1. Development of injectable dECM-enhanced hyaluronic microgels

2.2 Hyaluronic acid methacryloyl (HAMA) synthesis

HA powder (2.5 g) was dissolved in ultrapure water and stirred to dissolve. Subsequently, the pH value of the solution was adjusted to 8.5 with 1 M NaOH under ice bath conditions. Then, MA (5.6 mL) was added dropwise controlling the pH value at 7.5–8.5 for a duration of 4 h in an ice bath. The reaction system was stirred at room temperature overnight. After that, the solution was transferred to dialysis bags (Mw = 8000–14000 kDa) and dialyzed in ultrapure water for 3 days at room temperature to remove unreacted methacrylate groups. The dialysis solution was frozen and lyophilized to obtain HAMA. The chemical structure of HAMA was confirmed by H^1 NMR (400 MHz, Bruker AMX-400, USA) with D_2O as the solvent.

2.3 Preparation and characterization of dECM

Fresh porcine knee joints were collected, and the joint cavity was exposed to extract transparent cartilage pieces while avoiding calcified tissue. After ultrasonic cleaning in phosphate-buffered saline (PBS, Sigma Aldrich, USA), the cartilage pieces were lyophilized. Subsequently, the cartilage pieces were ground into particles using a cryogenic grinder at -20 ℃, 60 Hz and 3000 r/min. The obtained pellets were mixed with PBS, filtered through a 175 μm sieve, and then decellularized as the following steps reported previously [32, 33]. Firstly, the cartilage particles were alternately placed in hypotonic solution (10 mM Tris-HCI, pH = 8) and hypertonic solution (50 mM Tris-HCI, 1 M NaCl, pH = 8), repeated three times and performing five freeze–thaw cycles (liquid nitrogen and 37 °C water bath). After that, 1% CHAPS solution treatment for 5 h was applied to the cartilage ECM. Then, the obtained ECM was treated with nuclease solution (200 U/mL DNase I dissolved in 10 mM Tris-HCI, pH = 7.5) for 9 h at 37 °C with agitation, with a new solution replaced every 3 h. The ECM was next treated with 0.1% Triton-100 solution with agitation and washed several times with distilled water to remove residual detergent. Finally, the ECM powder was obtained by centrifugation and lyophilized. The powder was ground again through a 50 μm sieve and digested with 0.1 M acetic acid solution containing pepsin (pepsin: decellularized matrix = 1:10) for 2 days. The digestion was terminated by adjusting the pH to neutral to obtain the dECM solution stored at 4 ℃.

The typical components retained in the dECM were characterized as follows: 10 mg decellularized tissues was placed in 1 mL papain working solution and treated with a water bath at 65 ℃ overnight. After that, the supernatant was collected by centrifugation for the quantification of DNA and GAGs content by a Quant-iT PicoGreen dsDNA (B1302, Sigma) and the Blyscan glycosaminoglycan (GAG) assay kit (B100, Biocolor) in accordance with the outlined protocol. The dECM solution was applied to slides, air-dried for 30 min and then stained with hematoxylin–eosin (H&E) and toluidine blue (TB) according to the Hematoxylin–Eosin Staining Kit (G1120, Solarbio)

and the Toluidine Blue Staining Kit (G2543, Solarbio), respectively. The samples were then observed under a light microscope and photographed for subsequent analysis. The microstructure of decellularized tissues was observed by imaging using a scanning electron microscopy (SEM, Japan).

2.4 Preparation and characterization of HE hydrogel

HAMA (10 mg/mL) and dECM solution were mixed at a mass ratio of 1:2 to obtain the experimental group HE. Then the solution supplemented with photo-initiator was immediately injected into a homemade ring mold under light protection. Afterwards, the liquid crosslinked to form a gel under UV light (450 nm), and a series of material characterization was carried out in the subsequent process. The pure HAMA solution was formed into a gel in the same way as a control.

The lyophilized hydrogel was soaked in liquid nitrogen for a few seconds, followed by fracturing in a brittle manner to expose the cross-section, and the internal structure was observed by a scanning electron microscopy after gold coating treatment. The SEM images were analyzed using ImageJ software to obtain the porosity and pore size of the hydrogels.

The disintegration rate of the hydrogels was measured using hyaluronidase and type I collagenase solutions to simulate physiological conditions. The weight of fresh hydrogel was recorded as W_0. Then the samples were placed in PBS solutions containing type I collagenase (5 U/mL) and hyaluronidase (5 U/mL), respectively. Simultaneously they were placed in a thermostatic shaker at 90 rpm and 37 ℃. The fresh enzyme solution was replaced daily. The hydrogel was removed at certain time intervals, and the water on the surface was carefully wiped with filter paper to weigh(W_1). The weight measurement was repeated three times for each sample. The disintegration rate was calculated using the following formula:

$$\mathrm{WeightLoss} = (W0 - W1)/W0 * 100\%$$

Hydrogel swelling properties were measured as follows. Briefly, the initial weight of the lyophilized hydrogel was noted as W_0. The samples were immersed in PBS buffer and placed in a constant temperature shaker at 90 rpm and 37 °C. Finally, the hydrogels were periodically taken out and weighed noted as Ws. The weight measurement was repeated three times for each sample. Until the hydrogel swelling reached equilibrium, the swelling ratio was calculated using the following equation:

$$\mathrm{SwellingRatio} = (Ws - W0)/W0 * 100\%$$

In addition, fresh hydrogels were tested at room temperature using a Dynamic Mechanical Analyzer (DMA, TA-Q800, USA) under multi-frequency mode (a fixed frequency of 1–10 Hz, an amplitude of 40 μm, a preload force of 0.002 N and a force track of 105%) to test the energy storage modulus (G') and loss modulus (G"). Each sample was tested three times in parallel.

2.5 Preparation and characterization of microgels

The microfluidics device was utilized to prepare microgels with uniform size. Briefly, liquid paraffin oil was used as the continuous phase and Span 80 (5 wt% concentration) served as the surfactant to stabilize the droplets. The dispersed phase was composed of either a mixture of HAMA (1 wt% final concentration) and dECM (2 wt% final concentration), or a pure HAMA solution with a photo-initiator. Afterwards, the two phases were individually injected into different miro-channels of the device and the flow rates were adjusted by microfluidic pumps. The change in flow rates resulted in the size of microgels. An ultraviolet (UV) lamp placed above the channels ensured that microdroplets generated due to the shear stress of the continuous phase liquid formed solid hydrogels by photo-cross-linking at a constant rate within channels. The microgels were collected in a centrifuge tube at the outlet of the channel and purified by washing with acetone once and with PBS repeatedly to obtain HE and HA microgels.

The purified microgels were photographed under an optical microscope and the microgel particle size was analyzed using ImageJ software. SEM was used to observe the surface morphology of microgels. A certain amount of microgels was incubated in a PBS solution placed in a constant temperature shaker at 37 °C. At specific time points, an appropriate volume of the supernatant was collected to determine the release profile of each component from the microgels. Specifically, the collagen content was quantified using a hydroxyproline assay kit (Solarbio, BC0250), while IGF-1 (Bioswamp, Wuhan, PR40070), TGF-β1 (Bioswamp, Wuhan, PR40065), and BMP-2 (Bioswamp, Wuhan, PR40118) were measured using enzyme-linked immunosorbent assay (ELISA) kits to determine the levels of growth factors. Additionally, the GAG content was assessed using the Blyscan glycosaminoglycan (GAG) assay kit (B100, Biocolor).

2.6 Extraction and culture of OA chondrocytes

The articular cartilage was cleaned with PBS several times, cut into as thin and small pieces as possible and digested with EDTA-free trypsase for 0.5 h. The previous solution was then replaced and incubated with 2 mg/mL type II collagenase for 5 h. The P0-generation OA chondrocytes were obtained after passed through a 100 μm strainer and cultured in α-MEM medium with

the addition of 1% double antibody, 20% KEL serum, and 50 μg/mL VC. Once 90% confluence was reached, passaging was accomplished in 24-well plates (P1) for subsequent cell experiments.

2.7 *In vitro*effects of different microgels

2.7.1 Cell proliferation and morphology

The in vitro effects of microgels on OA chondrocytes were evaluated through a co-culture system within the Transwell apparatus. Microgels, prepared at a concentration of 1 mg/mL, were placed in the upper compartments of a 24-well Transwell plate, with OA chondrocytes seeded in the lower wells. The proliferation of OA chondrocytes, co-cultured with microgels for 3 and 7 days, was assessed using Live/dead cell staining and CCK-8. A PBS solution containing FDA/PI was added to the well plates and incubated in darkness for 5 min. Samples were then observed under a fluorescence microscope. Cell proliferation was detected using the CCK-8 kit, with the absorbance value of the incubation solution at 450 nm serving as the quantification metric. The cytoskeleton was stained with a Rhodamine-phalloidin solution to facilitate observation of cell morphology. Cells were washed thrice with PBS and soaked in 4% paraformaldehyde for 30 min at 4 ℃. Subsequently, cells were permeabilized with 0.1% Triton X-100 for 10 min and cleaned with PBS three times. These samples were then stained with a Rhodamine-phalloidin working solution (5 μg/mL) overnight at 4 ℃. Finally, cells were washed with PBS again and stained with a DAPI solution (10 μg/mL) for 1 min before observation under a fluorescence microscope. Photographs taken were analyzed by ImageJ software to obtain semi-quantitative data on cell spreading area and roundness.

2.7.2 Cellular matrix secretion

After culturing for 3 and 7 days, cartilage-specific polysaccharides secreted by OA chondrocytes were assessed by staining the cells with TB according to the Toluidine Blue Staining Kit (G2543, Solarbio). Semi-quantitative analysis of the staining images was done by ImageJ software. For quantitative GAG determination, OA chondrocytes in the well plates were collected after 3 and 7 days. The DNA and GAG quantitation were performed as mentioned in 2.4.1.

2.7.3 Chondrogenic phenotypes

To analyze RNA expression, OA chondrocytes after 5 days of co-culture with microgels were collected in RNA Later water and stored at -20 °C. The cellular RNA was extracted with RNeasy Mini Kit (74,104, Qiagen) and the concentration was detected by the microspectrophotometer (ND1000, Nanodrop Technologies). Next, RNA was reversed transcription (RT) extracted to cDNA using the iScript™ cDNA Synthesis Kit (BIO-RAD). The polymerase chain reaction (PCR) reaction was conducted on the CFX96 Touch™ Real-Time Fluorescent PCR Detection System (BIO-RAD). The expression levels of cartilage matrix-related genes (GAPDH, COL I, COL II, COL X, SOX9 and Aggrecan) in OA cells were determined using GAPDH as an internal reference. The primers are shown in Table S1.

2.8 *In vivo* effects of different microgels

2.8.1 Establishment of an OA rat model

The procedures adhered to the current guidelines for the care of experimental animals. Male SD rats, aged 6–8 weeks and weighing approximately 250 g, were selected for the establishment of the osteoarthritis model. The rats were anesthetized with an intraperitoneal injection of 2% sodium pentobarbital (2 mL/kg), and the anterior cruciate ligament in the knee joint cavity was disrupted using previously reported methods, namely anterior cruciate ligament transverse (ACLT) [34]. Four weeks later, intra-articular injections of 100 μL of PBS, or PBS mixed with a 10 mg/mL concentration of HA or HE microspheres ranging from 80 to 85 μm, were randomly administered to osteoarthritic rats. The meanings of the group names are as follows: NA: as well as Native, healthy rats; PBS: rats treated with PBS solution; HA: rats treated with HA microgels; HE: rats treated with HE microgels.

2.8.2 Radiographic assessment

Four weeks post-injection, Micro-CT scans were performed on the knee joints of the osteoarthritic rats, and images were reconstructed based on the scanned data. The knee width and joint space width were also semi-quantitatively analyzed in each group.

2.8.3 Histologic evaluation

The rats were executed by over-anesthetized after four weeks of sample injection, and the collected articular joints were photographed to observe the width of the articular synovial cartilage. The gross appearance was scored according to the scoring criteria (Table S2) [35]. The knee joints were immersed in a 4% paraformaldehyde solution for 1 week, decalcified with EDTA solution at 37 ℃, embedded in paraffin, and sectioned. The sections underwent H&E staining, TB staining, Masson staining, and Sirius Red staining to analyze the histological characteristics of the tissues. The severity of osteoarthritis in each group of specimens was assessed based on the staining results, with reference to the Mankin histological score (Table S3). Subsequently, the sections were immunologically stained using antibodies against type I collagen and type II collagen, following the protocols of the antibody kits.

2.9 Statistical analysis

Statistical analysis was performed using GraphPad Prism 8 software, and multiple t-tests were used to analyze inter- and intra-group differences. Data results were expressed as mean ± standard error (SE) and mean ± standard deviation (SD) for at least three samples per test, with p values indicating statistically significant results ($^{*}p < 0.05$, $^{**}p < 0.01$ and $^{***}p < 0.001$).

3 Results and discussion

3.1 Preparation and characterization of dECM

The decellularization of fresh porcine cartilage slices was prepared by optimizing the previously established decellularized cartilage ECM preparation protocol. This involved performing multiple grinding and sieving to retain small-sized particles, thereby eliminating cells and preserving tissue-specific components as much as possible. As shown in Fig. 1A, for further preparation of the composite hydrogel, the dECM particles were digested into the solution by pepsin to be co-mingled with HAMA to form a gel. DAPI, H&E, and TB staining, as well as the results of microstructural images and semiquantitative analyses (Fig. 1B, C) demonstrated that there were virtually no cells in the dECM as compared to fresh natural cartilage. The success of decellularization was further confirmed through DNA quantitative analysis, revealing the removal of approximately 98% of immunogenic cellular components. The remaining DNA concentration in dECM was 44.30 ± 0.51 ng/mg tissue weight, which is below the critical decellularization criterium of 50 ng/mg (Fig. 1D) [36]. Critical components of the ECM were characterized before and after decellularization. Despite the decellularization process inevitably results in the loss of ECM components, collagen, with its

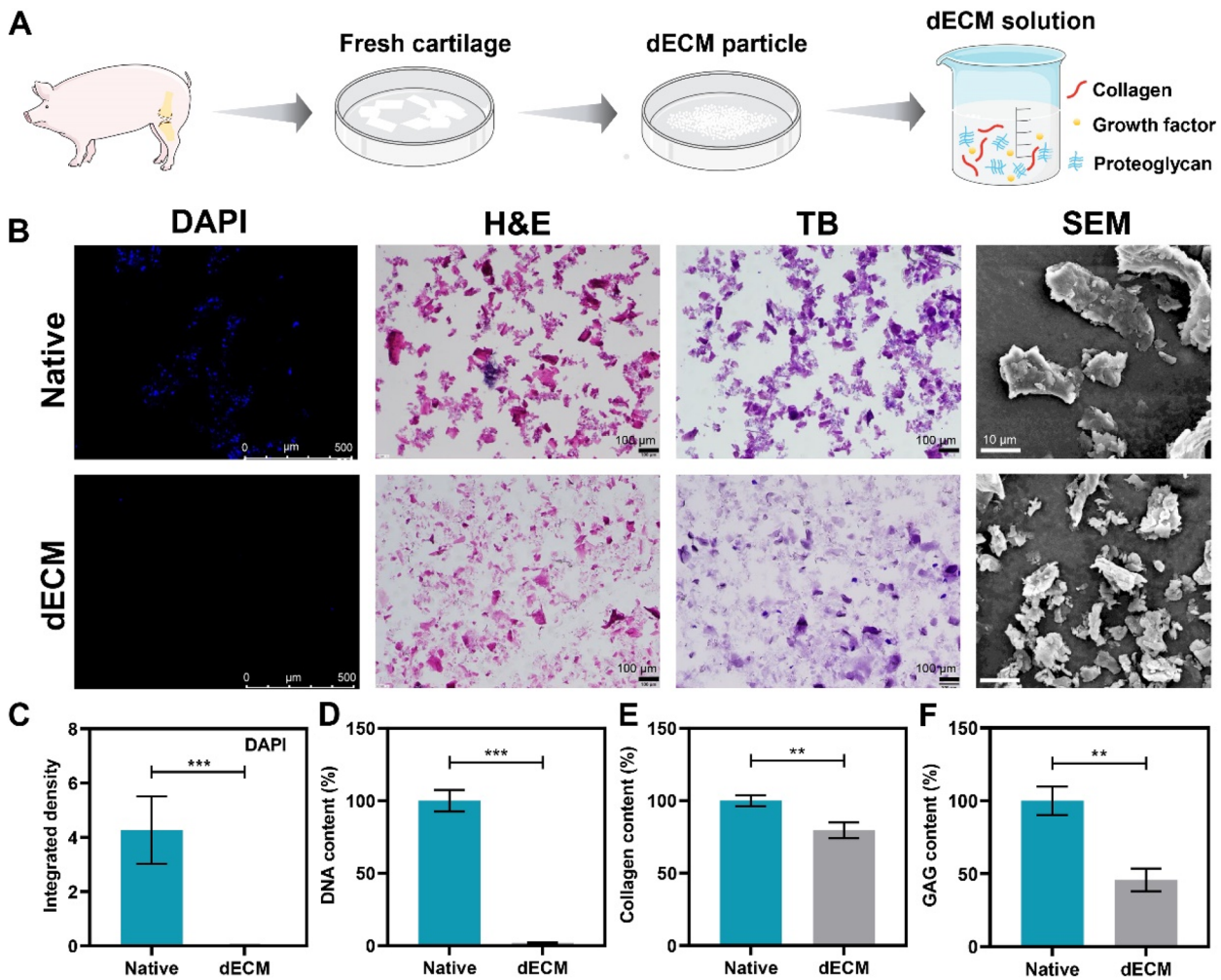

Fig. 1 (**A**) Scheme of decellularized cartilage ECM preparation. (**B**) Representative DAPI, histologic staining of H&E staining, TB staining and SEM images of native ECM and dECM. (**C**) Semi-quantitative determination of DAPI. (**D**) DNA, (**E**) Collagen, (**F**) GAG contents of native ECM and dECM. Error bars represent SD ($n \geq 3$). $*p < 0.05$, $**p < 0.01$, $***p < 0.001$

large molecular size, intermolecular entanglement, and relatively low solubility, exhibited a high retention rate of approximately 80% after decellularization (Fig. 1E). GAG quantification showed that after the decellularization process, approximately 45% of GAG was retained (Fig. 1F).

3.2 Preparation and characterization of HE hydrogels

HAMA was synthesized by grafting methacrylic anhydride onto HA, and the chemical structure was determined by ^{1}H NMR as shown in Fig. S1. Distinct new resonant peaks at 5.8 and 6.2 ppm in the HAMA spectra confirmed the existence of the methacryloyl group suggesting that the hyaluronic acid has been modified by methacrylic anhydride. In combination of HA and cartilage-derived dECM, it formed HE hydrogels to mimic the physiological extracellular matrix (Fig. 2A). The microstructure of hydrogels was observed by scanning electron microscopy (Fig. 2B, C). They both presented an interconnected porous structure, which facilitated nutrient transfer and cell migration and proliferation. The addition of dECM significantly decreased the pore size and porosity of the HE hydrogels compared to the control. DMA results showed that the storage and loss modulus of the HE hydrogels were higher than those of the HA group as the frequency increased. This indicated a significant enhancement in mechanical properties due to the incorporation of dECM (Fig. 2D, E). The degradation behavior of hydrogels was evaluated by two enzyme solutions (Fig. 2F, G). In the hyaluronidase solution, the rate of HA loss was higher, suggesting that dECM could slow down the degradation rate of the material and effectively alleviate the problem of short retention time of HA in intra-articular injection therapy. In PBS buffer, the hydrogels rapidly reached solubilization equilibrium and exhibited excellent water absorption and retention properties (Fig. 2H). The dual-network hydrogel structure formed by the addition of dECM to HA was conducive to delaying the release of the active ingredients of dECM, especially the large molecular weight components, such as GAG and collage, realizing its sustained effect on the recovery of chondrocyte phenotype and cartilage reconstruction.

3.3 Preparation and characterization of HE microgels

To improve intra-articular injectability for the treatment of osteoarthritis, the HE microgels were fabricated using microfluidics devices. As shown in Fig. 3A, the continuous phase enters the channel from both sides, generating and encapsulating the dispersed-phase droplets under the shear forces of the continuous phase. These droplets are then cured by a UV light source above the collection channel. Upon determining the material concentration, the flow rate ratio of the continuous and dispersed phases was adjusted by a syringe pump, resulting in a corresponding change in the diameter of the microgels. In this study, the flow rate ratio of the continuous and dispersed phases was set at 10:1. This resulted in HE microgels with a uniform size distribution and an average particle size ranging from 80–85 μm. This ensured that the microgels could pass through a 1 mL syringe (with an inner diameter of 0.25 mm) without disrupting their morphology, thereby ensuring good injectability (Fig. 3B). Under microscopic observation, the microgels were dispersed in a regular spherical shape. For better observation, a dye solution was added dropwise to the solution, revealing that the dECM was uniformly distributed within the microgels. The microscopic morphology of the microgels was further studied using scanning electron microscopy, as shown Fig. 3C. The incorporation of dECM enhanced the composition of microgels with a diverse range of growth factors, as well as GAG, and collagens. These components play crucial roles in the cellular behavior of chondrocytes, such as proliferation, morphology and matrix secretion. The release profiles of key growth factors, such as IGF-1, TGF-1β, and BMP-2, and the cartilage-specific structural macromolecules and proteins, including GAG and collagen, in both microgels were evaluated. The release curves demonstrated that approximately 60% of the small molecular weight growth factors were released within 7 days (Fig. 3D-F), while the water-soluble GAG exhibited a slower release trend due to the formation of a network structure through HA cross-linking (Fig. 3G). Consequently, the structural collagen with high molecular weight demonstrated the slowest release rate (Fig. 3H), and its releasing behavior in hyaluronidase condition suggested that its gradual release is dependent on the degradation of microgels (Fig. 3I). The release of growth factors, structural ECM macromolecules and proteins showed a significant temporal correlation, indicating that microgels possess biomimetic properties for actively modulating the dynamic microenvironment during cartilage formation.

3.4 HE microgels enhance proliferation and morphology of OA chondrocytes

To observe the effects of both microgels on cell proliferation and morphology, transwell chambers were utilized to co-culture microgels with OA chondrocytes in vitro (Fig. 4A). The viability and proliferation of OA chondrocytes were assessed by live/dead staining result (Fig. 4B) and CCK-8 assay (Fig. 4C). The results collectively demonstrated that the addition of HE microgels significantly increased the proliferative activity of OA chondrocytes. Notably, at 3 days, the difference between the HE group and the remaining groups was the most significant, accompanied

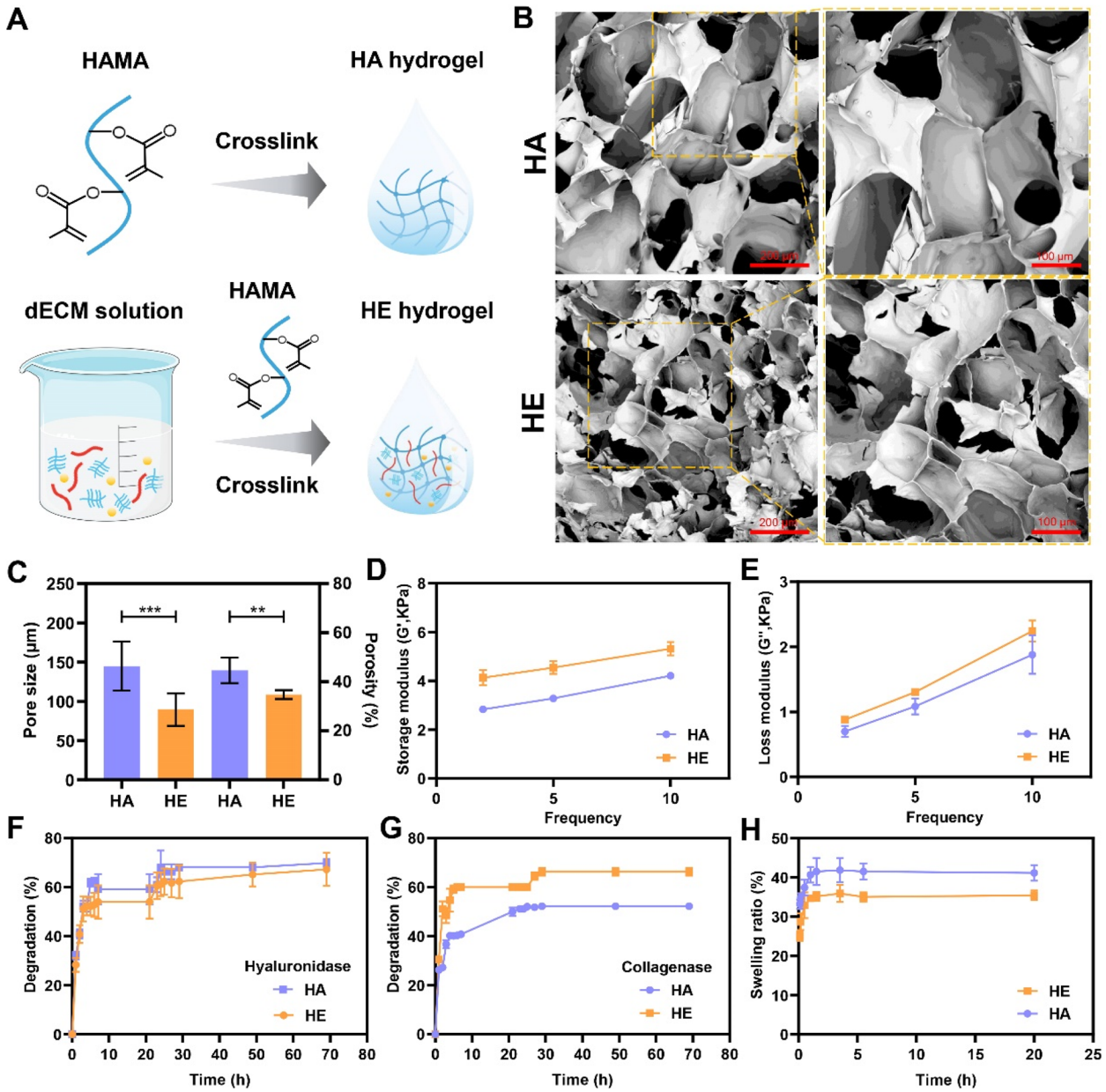

Fig. 2 (**A**) Scheme of hydrogel constituents. (**B**) Hydrogel microstructure (SEM). (**C**) Pore size and porosity of hydrogels. (**D**) Storage and **E** loss modulus of hydrogels. (**F**-**G**) Degradation behavior of hydrogels in two enzyme solutions. (**H**) Solubilization properties of hydrogels. Error bars represent SD ($n \geq 3$). $*p < 0.05$, $**p < 0.01$, $***p < 0.001$

by a pronounced increase in cell number. This may be attributed to the rapid release of growth factors such as IGF-1, TGF-1β, and BMP-2 from HE hydrogels, which recover OA chondrocytes' function to boost proliferation. OA chondrocytes exhibited irregular cell morphology and hypertrophy in in vitro culture. The ability of HE microgels to promote morphological recovery of OA chondrocytes with increasing co-culture time was indicated by rhodamine/DAPI staining (Fig. 4D), as well as semi-quantitatively by spreading area (Fig. 4E1) and cell roundness (Fig. 4E2). At 3 days, with the rapid release of growth factors from the HE microgels, the larger cell spreading area of OA chondrocytes corresponded to enhanced proliferation, consistent with the CCK-8 data. The decrease in spreading area and cell roundness of OA chondrocytes in the HE group at 7 days may indicate the synergetic effects of the continuously released growth factors and the slow-released dECM macromolecules on the recovery of cell morphology.

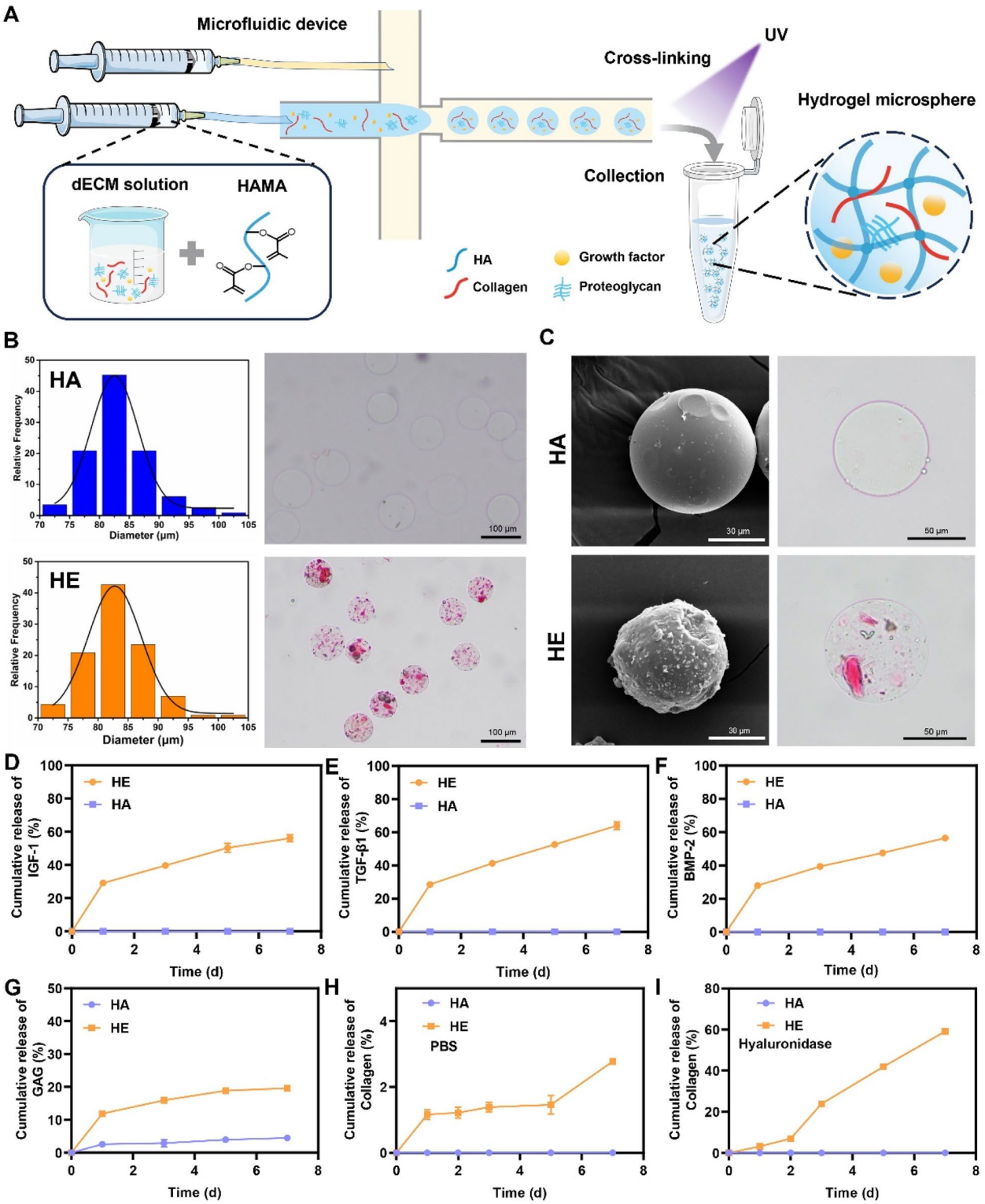

Fig. 3 (**A**) Schematic diagram of the protocol for the preparation of microgels by microfluidics. (**B**) Particle size distribution of two kinds of microgels. (**C**) SEM images as well as representative light microscopy images of the two microgels. Release curve of **D** IGF-1, **E** TGF-1β, **F** BMP-2, **G** GAG, and **H**, **I** collagen from microgels

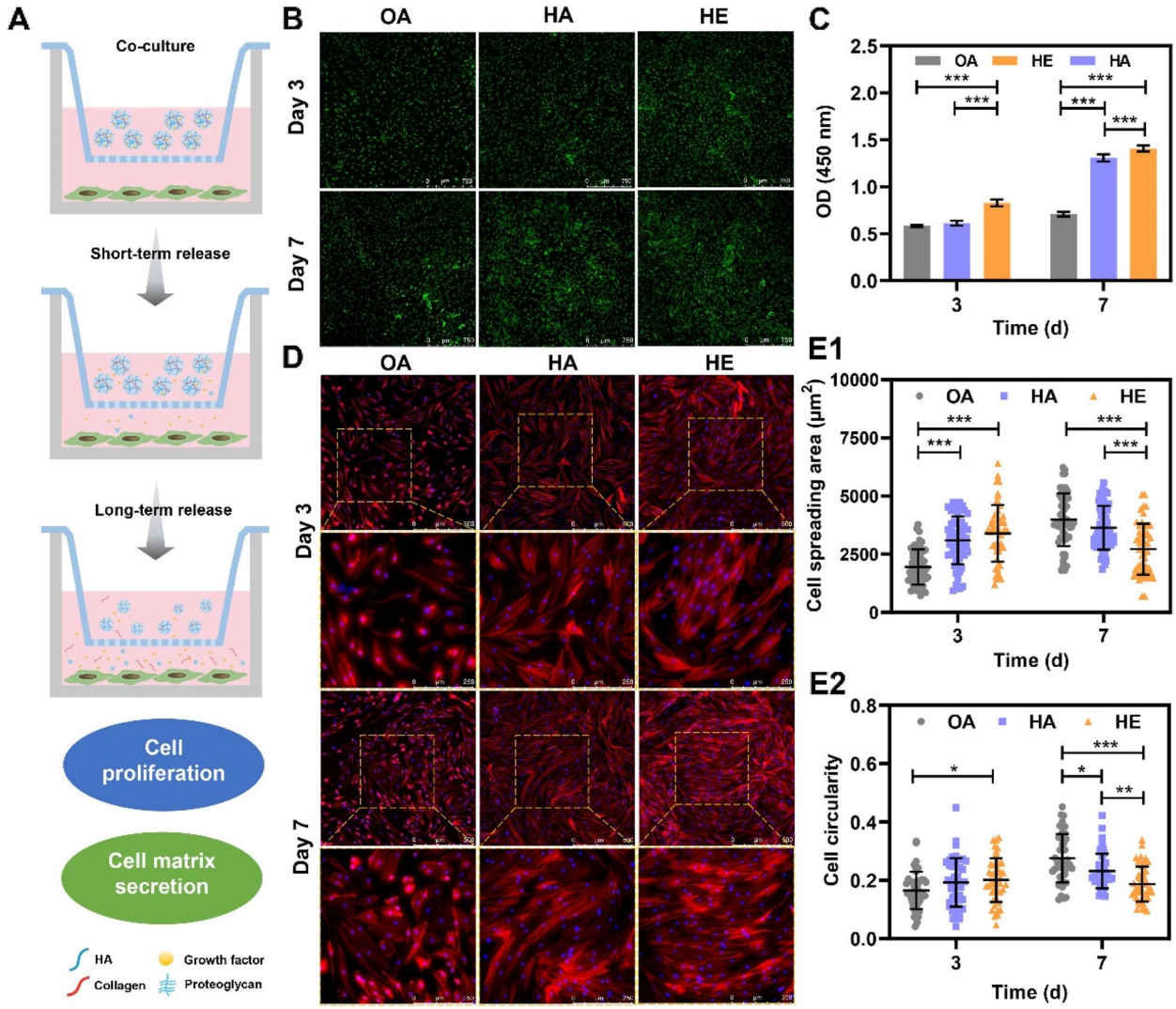

Fig. 4 (**A**) Schematic diagram of co-culture method assessing interactions between porous microgels and cells in vitro. (**B**) Live/dead staining images of OA cells after 3 and 7 days of co-culture. (**C**) Measurement of OA cell proliferation by CCK-8 kit. (**D**) Cytoskeleton staining after 3 and 7 days of co-culture, cell spreading area (E1), cell circularity (E2). Error bars represent SD ($n \geq 3$). $*p < 0.05$, $**p < 0.01$, $***p < 0.001$

3.5 HE microgels promote cartilage matrix secretion of OA chondrocytes

GAG is a crucial component of cartilage ECM and serves as an indicator for assessing the chondrocytes' function in cartilage regeneration and homeostasis. The ability of HE microgels to regulate cartilage ECM secretion in OA chondrocytes was further investigated. The HE group exhibited superior pro-chondrogenic matrix secretion in OA chondrocytes compared to the HA group (Fig. 5A), as evidenced by stronger positive staining from toluidine blue (TB) staining after 3 and 7 days of co-culture, corroborated by semi-quantitative data (Fig. 5B). HE microgels contributed to an increase in cell number and enhancement of cartilage-specific polysaccharide synthesis, as shown in the quantitative analysis of DNA and GAG (Fig. 5C-E). The regulatory effect of HE microgels on cartilage matrix synthesis in OA chondrocytes was not significantly evident at 3 days, suggesting that the observed effect during this time period may be primarily attributed to enhanced proliferation based on the CCK-8 data. However, the GAG/DNA values of the HE group significantly surpassed those of the other groups at 7 days, providing further evidence for the enhancement of matrix synthesis by growth factors and degradation products. In addition, the qPCR assessed the expression of various cartilage-specific genes in OA chondrocytes after 5 days of co-culture with microgels (Fig. 5F): the expression of COL I

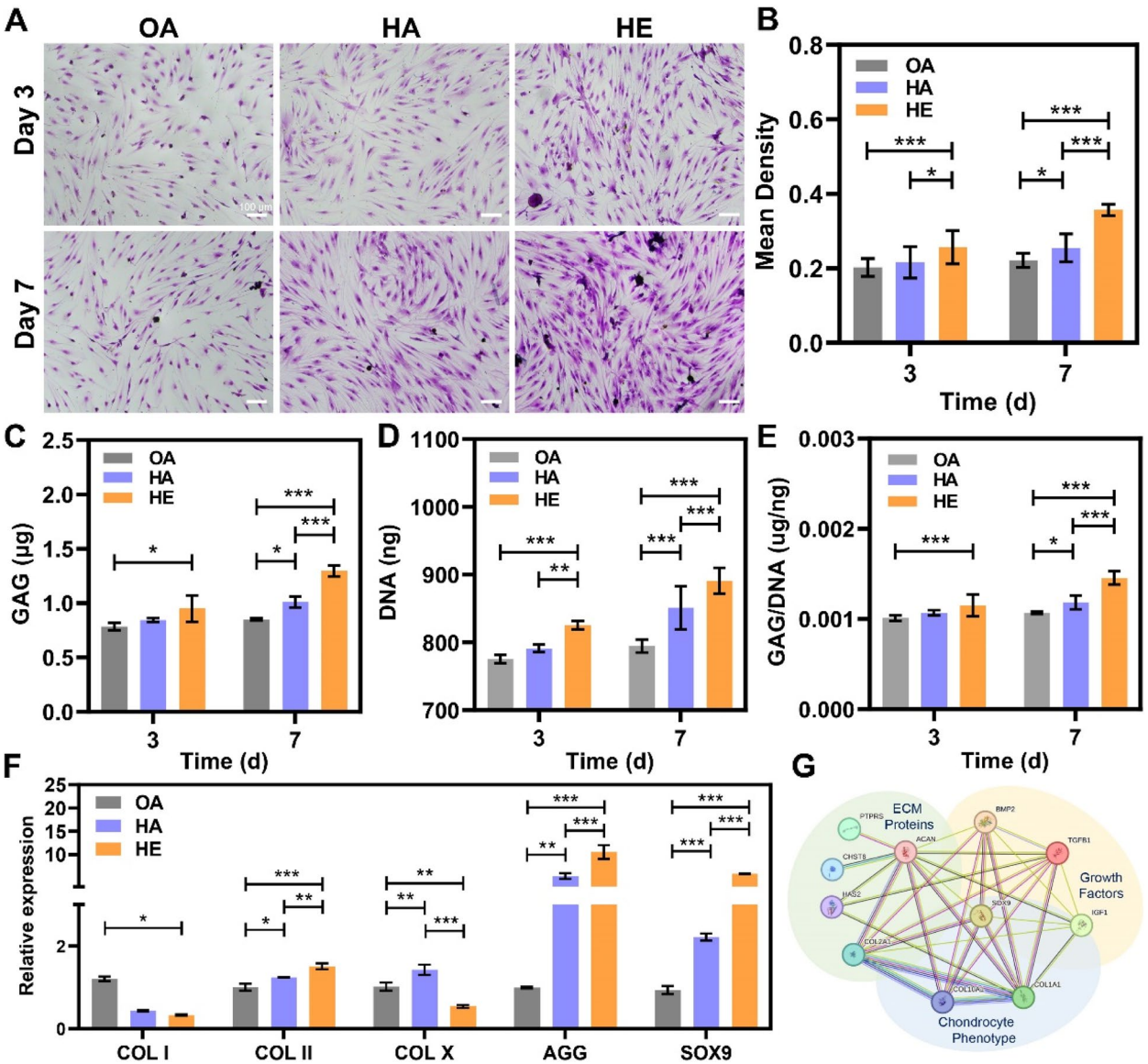

Fig. 5 (**A**) Toluidine blue staining images and **B** semi-quantitative results of OA chondrocytes after 3 and 7 days of co-culture. (**C**) GAG, **D** DNA, and **E** GAG/DNA quantification. (**F**) Expression levels of cartilage matrix-related genes in OA chondrocytes co-cultured for 5 days. (**G**) Plot of the relationship between ECM proteins genes, growth factors genes and cartilage phenotype related genes. Error bars represent SD ($n \geq 3$). $*p < 0.05$, $**p < 0.01$, $***p < 0.001$

gene was associated with chondrogenic fibrosis, COL II and AGG represented ECM synthesis, COL X gene was expressed in chondrocyte hypertrophy, and SOX9 was the essential cartilage-promoting factor, which can alleviate the progression of OA. HE microgels significantly decreased the expression level of COL I and COL X genes and significantly increased the expression of COL II, AGG, and SOX9. This finding was further supported by the close relationship among the three key growth factors and the structural ECM macromolecules towards the chondrocyte's phenotype, based on the gene interaction network map generated using the STRING database (Fig. 5G). In summary, HE microgels demonstrated enhanced secretion of cartilage matrix and expression of cartilage-specific genes in OA chondrocytes in vitro, as evidenced by histological staining, GAG/DNA analysis, and gene expression levels. This can be attributed to the synergistic effect of spatiotemporal release of cartilage-specific molecules, which rapidly recover the function of OA chondrocytes with the short-term release of cartilage-specific growth factors, and continuously support the cartilage regeneration and homeostasis with the long-term release of

structural ECM macromolecules and proteins, such as GAGs and collagens, as the HE microgels degrades.

3.6 *In vivo* evaluation of HE microgels for OA alleviation

The therapeutic potential of HE microgels for OA alleviation was evaluated using a rat OA model established by ACLT surgery. Different samples were injected into the joint cavity four weeks post-surgery (Fig. 6A), and the joints were reconstructed using micro-computed tomography (micro-CT) to assess the OA progression. The subchondral bone treated with PBS was found to be severely deformed, with a concave and uneven surface. In contrast, the joints

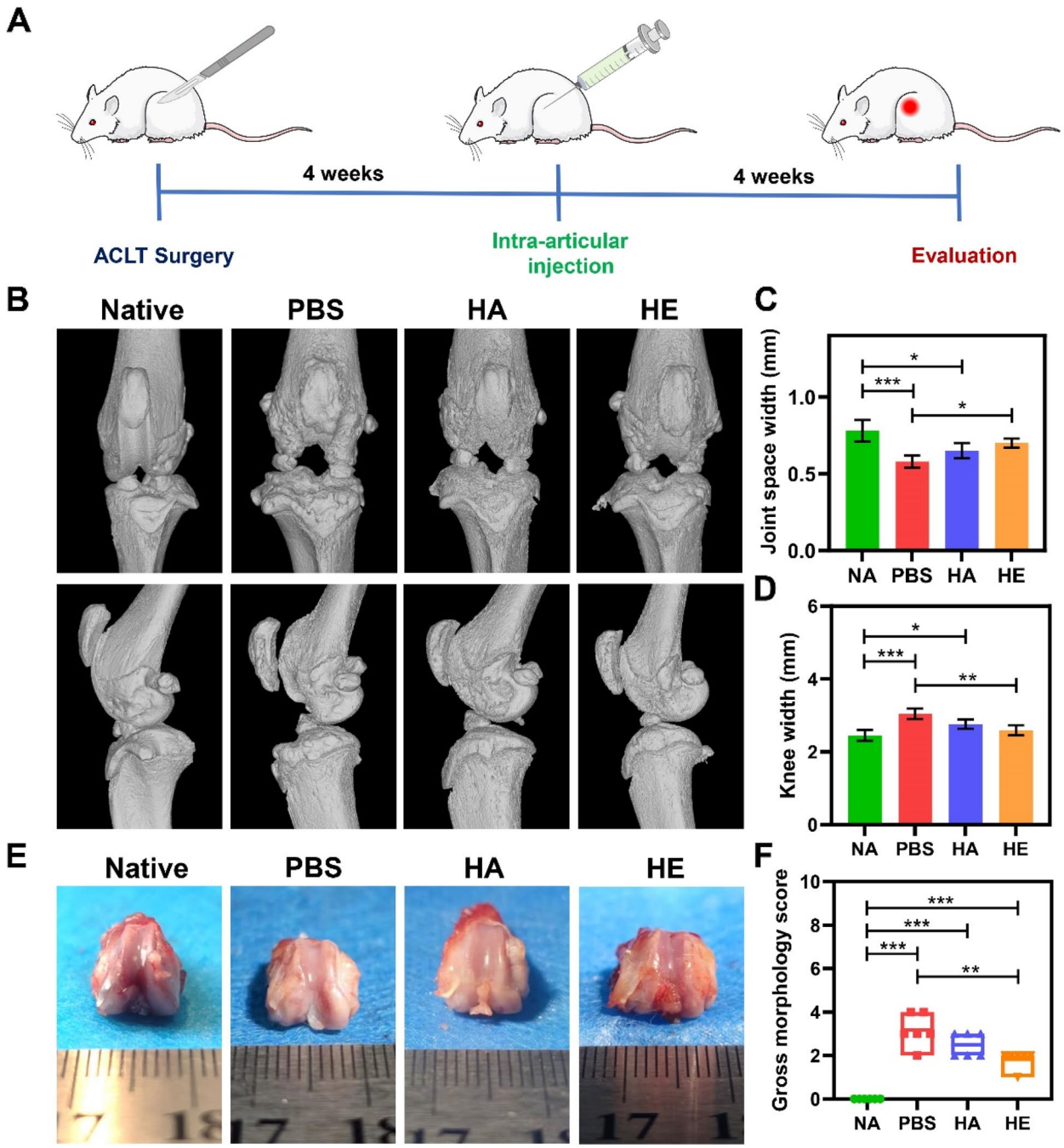

Fig. 6 (**A**) Scheme of evaluating the effect of microgels in OA rat models. (**B**) micro-CT, (**C**) joint space width and **D** knee width of samples. (**E**) gross appearance of the keen joints four weeks after sample injection and **F** gross morphology score. Error bars represent SD ($n = 6$). $*p < 0.05$, $**p < 0.01$, $***p < 0.001$

treated with HE microgels more closely resembled the morphology and structure of healthy rat joints (Fig. 6B). According to semi-quantitative knee analysis (Fig. 6C, D), there was no statistical difference between the HE microgel treatment and the native group (NA). A decrease in joint space width reduction and maintenance of knee width suggest that HE microgels attenuate osteoarthritic degeneration after four weeks of injection [37]. The gross view of the knee joint (Fig. 6E) and the gross morphology score (Fig. 6F) were consistent with the joint visualization results, suggesting the effectiveness of the treatment.

The H&E staining of the natural joints showed neat and orderly chondrocyte arrangement, a homogeneous matrix, and a smooth surface of the cartilage layer (Fig. 7A). In

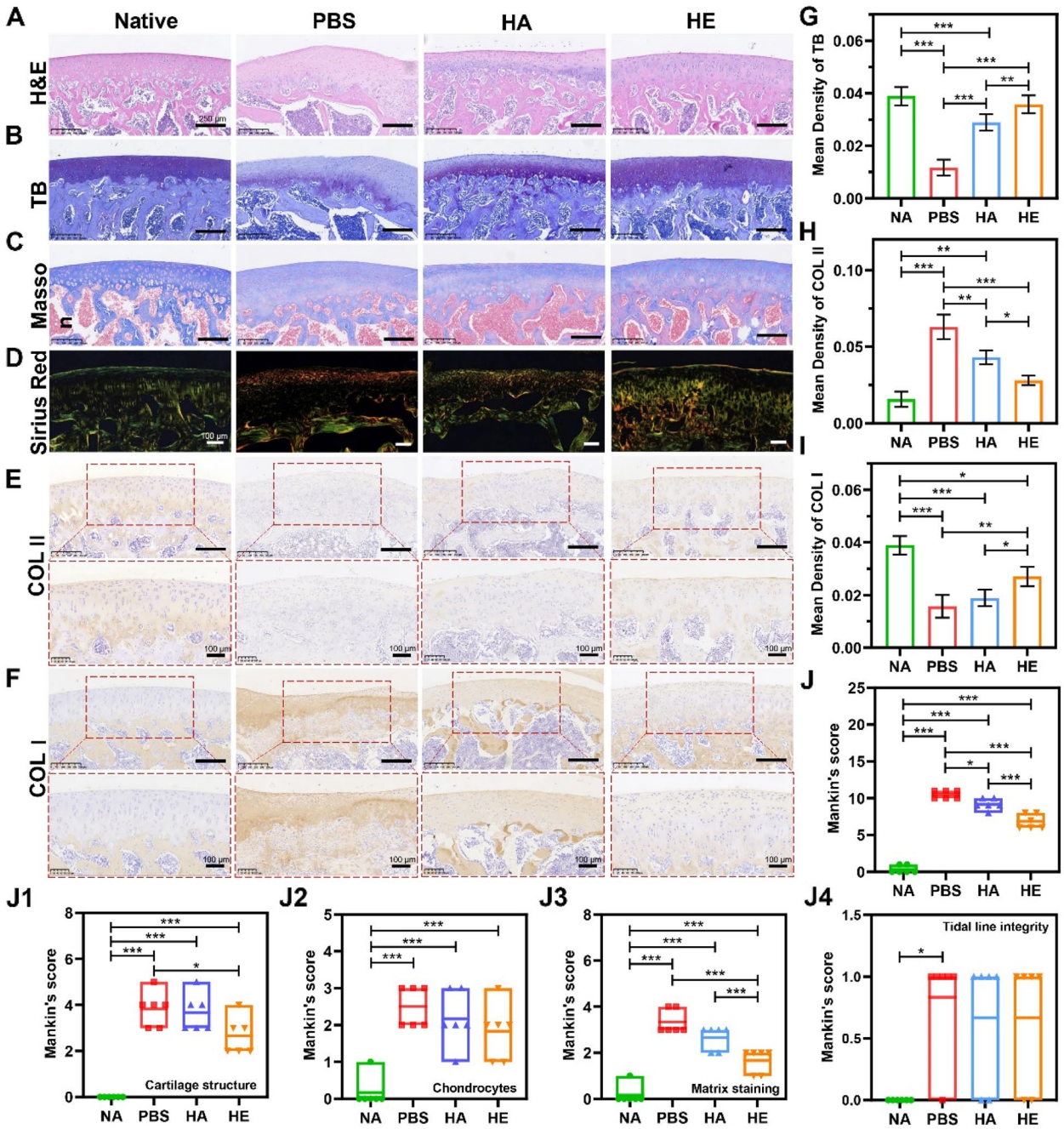

Fig. 7 Four weeks after intra-articular injection, tissue sections of rat OA knee joints were stained for **A** H&E, **B** TB, **C** Masson, **D** Sirius Red, **E** COL II, and **F** COL I. Semi-quantitative analysis of **G** TB, **H** COL II, and **I** COL I staining, **J** Mankin histologic scores for cartilage structure, chondrocyte, matrix staining and tidal line integrity ($n=6$). $*p<0.05$, $**p<0.01$, $***p<0.001$

contrast, the PBS group exhibited significant tissue fibrosis, disorganized cell arrangement, and an uneven cartilage layer. Despite the lubricating effect of HA leading to a smoother surface, the HA-treated group displayed a reduction in thickness and lighter staining color matrix layer along with irregularly arranged cells. This suggests that HA's ability to effectively repair damaged cartilage tissue is limited. On the other hand, the HE group showed a significant improvement in both cell arrangement and matrix, which can be attributed to the combined lubricating properties of HA and the cartilage matrix synthesizing function of dECM. Furthermore, the TB (Fig. 7B), Masson (Fig. 7C), Sirius Red (Fig. 7D) staining and semi-quantitative analysis (Fig. 7G) allowed for a general assessment of GAG levels. Among the experimental groups, representative images of the HE group demonstrated the superior results by best preserving the GAGs and minimizing the fibrocartilage production in the regenerated cartilage matrix. In addition, COL I and II, classic indicators representing the quality of regenerated cartilage, were assessed by immunohistochemical staining (Fig. 7E, F) and semiquantitative data (Fig. 7H, I) to further evaluate the quality of neocartilage tissues. The HE group exhibited significantly higher production of COL II with minimal level of COL I, indicating its superiority in the regeneration of healthier hyaline cartilage. Based on above observations, Mankin histological scores (Fig. 7J) were utilized to illustrate the differences between the experimental groups and the natural group in terms of cartilage structure, chondrocytes, matrix staining, and tidemark integrity. The results suggested that the HE groups had achieved the significant improvements over the PBS and HA groups in the overall Mankin score, with distinct amelioration in OA cartilage structure and matrix staining. Collectively, HE microgels effectively promoted the repair of articular cartilage and significantly alleviated the degree of OA, evidenced by radiological observation, gross appearance, histological/immunohistochemical staining, and analysis in an OA rat model in vivo.

4 Conclusion

This study successfully pioneered a cell-free OA therapy approach, utilizing intra-articular injectable dECM-enhanced HA microgels. These microgels, characterized by their uniform size and mechanical strength, were fabricated using microfluidics and photopolymerization. They provided a spatiotemporal cascade effect, enabling the rapid release of cartilage-specific growth factors such as IGF-1, TGF-β, and BMP-2. This facilitated the swift recovery of OA chondrocytes' function. Simultaneously, the slower release of cartilage structural ECM macromolecules and proteins, including GAGs and collagens, continuously supplied essential elements for supporting cartilage regeneration and homeostasis as the microgels degraded. This enhancement was observed in terms of cell proliferation, morphology, matrix synthesis, and cartilage-specific gene expression. Furthermore, HE microgels effectively promoted the regeneration of collagen II-enriched hyaline cartilage and significantly alleviated the degree of OA, evidenced by radiological observation, gross appearance, histological/immunohistochemical staining, and analysis in an OA rat model in vivo. Together, it underscores the potential of HE microgels in dECM combined with HA as a promising therapeutic approach for OA.

Abbreviations

OA	Osteoarthritis
HE	DECM-enhanced hyaluronic
NSAIDs	Non-steroidal anti-inflammatory drugs
HA	Hyaluronic acid
ECM	Extracellular matrix
dECM	Decellularized ECM
TGF-β	Transforming growth factor-β
IGF-1	Insulin-like growth factor-1
BMP	Bone morphogenetic protein
FGF	Fibroblast growth factor
EGF	Epidermal growth factor
MA	Methacrylic anhydride
CHAPS	3-[(3-Cholamidopropyl) dimethylamino] propanesulfonic acid internal salt
HAMA	Hyaluronic acid methacryloyl
GAG	Glycosaminoglycan
H&E	Hematoxylin–eosin
TB	Toluidine blue

Supplementary Information

The online version contains supplementary material available at https://doi.org/10.1186/s42825-024-00158-6.

Supplementary Material 1.

Acknowledgements

We would like to thank Sichuan University Analysis & Testing Center for technical assistance with Micro-CT.

Authors' contributions

SYD designed this project and revised the manuscript. SYD, HFC, YL and WQS performed experiments and analyzed data. MYC and XLC performed experiments and draw the scheme. JL, YJF, QGW and XDZ reviewed the manuscript. All authors read and approved the final manuscript.

Funding

This work was supported by the National Key Research Program of China (2023YFB4605800), the Natural Science Foundation of China (32071353) and the 111 Project (B16033).

Availability of data and materials

All data generated or analyzed during this study are presented in this article.

Declarations

Ethics approval and consent to participate

Human OA articular cartilage tissue was obtained from total joint replacement surgery under the ethical support of the Biomedical Ethics Review Committee of West China Hospital, Sichuan University (2022200). The animal experiments were approved by the Ethical Committee of Sichuan University (KS2020308). All the animals were purchased from Laboratory Animal Center of Sichuan University. The animal experiment guidance from the ethical committee and

the guide for care and use of laboratory animals of Sichuan University were followed during the whole experiment course.

Competing interests
The authors declare that they have no known competing financial interests or personal relationships that could have appeared to influence the work reported in this paper.

Author details
[1]National Engineering Research Center for Biomaterials, Sichuan University, Chengdu, Sichuan 610065, China. [2]College of Biomedical Engineering, Sichuan University, Chengdu, Sichuan 610065, China. [3]School of Medicine, The Chinese University of Hong Kong, Shenzhen 518172, China. [4]Department of Orthopedic Surgery & Musculoskeletal Medicine, Centre for Bioengineering & Nanomedicine, University of Otago, Christchurch 8011, New Zealand. [5]Sichuan Testing Center for Biomaterials and Medical Devices Co.Ltd, 29 Wangjiang Road, Chengdu, Sichuan, China.

Received: 18 January 2024 Revised: 21 March 2024 Accepted: 24 March 2024
Published online: 01 June 2024

References

1. Cui A, Li H, Wang D, Zhong J, Chen Y, Lu H. Global, regional prevalence, incidence and risk factors of knee osteoarthritis in population-based studies. EClinicalMedicine. 2020;29–30:100587.
2. da Costa BR, Pereira TV, Saadat P, Rudnicki M, Iskander SM, Bodmer NS, et al. Effectiveness and safety of non-steroidal anti-inflammatory drugs and opioid treatment for knee and hip osteoarthritis: network meta-analysis. Br Med J. 2021;375:n2321.
3. Zhang W, Moskowitz RW, Nuki G, Abramson S, Altman RD, Arden N, et al. OARSI recommendations for the management of hip and knee osteoarthritis, Part II: OARSI evidence-based, expert consensus guidelines. Osteoarthritis Cartilage. 2008;16(2):137–62.
4. Tommaso I, Daniele L, Beniamino P. Intra-articular injections for the treatment of osteoarthritis focus on the clinical use of hyaluronic acid. Drugs R D. 2011;11(1):13–27.
5. CatNTC C. Vascular and upper gastrointestinal effects of non-steroidal anti-inflammatory drugs: meta-analyses of individual participant data from randomised trials. Lancet. 2013;382(9894):769–79.
6. Kou L, Xiao S, Sun R, Bao S, Yao Q, Chen R. Biomaterial-engineered intra-articular drug delivery systems for osteoarthritis therapy. Drug Deliv. 2019;26(1):870–85.
7. Watterson JR, Esdaile JM. Viscosupplementation: therapeutic mechanisms and clinical potential in osteoarthritis of the knee. J Am Acad Orthop Surg. 2000;8(5):277–84.
8. Lucke M, Messner W, Kim ESH, Husni ME. The impact of identifying carotid plaque on addressing cardiovascular risk in psoriatic arthritis. Arthritis Res Ther. 2016;18:1733.
9. Fakhari A, Berkland C. Applications and emerging trends of hyaluronic acid in tissue engineering, as a dermal filler and in osteoarthritis treatment. Acta Biomater. 2013;9(7):7081–92.
10. Maudens P, Meyer S, Seemayer CA, Jordan O, Allémann E. Self-assembled thermoresponsive nanostructures of hyaluronic acid conjugates for osteoarthritis therapy. Nanoscale. 2018;10(4):1845–54.
11. Stellavato A, dE Novellis F, Reale S, De Rosa M, Schiraldi C. Hybrid complexes of high and low molecular weigth: Evaluation using an in vitro model of osteoarthritis. J Biol Regul Homeost Agents. 2016;30(4):7–15.
12. Lin X, Tsao CT, Kyomoto M, Zhang M. Injectable natural polymer hydrogels for treatment of knee osteoarthritis. Adv Healthc Mater. 2021;11(9):2101479.
13. Atwal A, Dale TP, Snow M, Forsyth NR, Davoodi P. Injectable hydrogels: An emerging therapeutic strategy for cartilage regeneration. Adv Colloid Interface Sci. 2023;321:103030.
14. Tezel A, Fredrickson GH. The science of hyaluronic acid dermal fillers. J Cosmet Laser Ther. 2008;10(1):35–42.
15. Seong Y-J, Lin G, Kim BJ, Kim H-E, Kim S, Jeong S-H. Hyaluronic acid-based hybrid hydrogel microspheres with enhanced structural stability and high injectability. ACS Omega. 2019;4(9):13834–44.
16. Lei Y, Wang Y, Shen J, Cai Z, Zhao C, Hong C, et al. Injectable hydrogel microspheres with self-renewable hydration layers alleviate osteoarthritis. Sci Adv. 2022;8(5):eab16449.
17. Yu H, Huang C, Kong X, Ma J, Ren P, Chen J, et al. Nanoarchitectonics of cartilage-targeting hydrogel microspheres with reactive oxygen species responsiveness for the repair of osteoarthritis. ACS Appl Mater Interfaces. 2022;14(36):40711–23.
18. Cunniffe GM, Díaz-Payno PJ, Sheehy EJ, Critchley SE, Almeida HV, Pitacco P, et al. Tissue-specific extracellular matrix scaffolds for the regeneration of spatially complex musculoskeletal tissues. Biomaterials. 2019;188:63–73.
19. Jiang W, Zhang X, Yu S, Yan F, Chen J, Liu J, et al. Decellularized extracellular matrix in the treatment of spinal cord injury. Exp Neurol. 2023;368:114506.
20. Wang X, Lu Y, Wang W, Wang Q, Liang J, Fan Y, et al. Effect of different aged cartilage ECM on chondrogenesis of BMSCs in vitro and in vivo. Regen Biomater. 2020;7(6):583–95.
21. Peng Z, Sun H, Bunpetch V, Koh Y, Wen Y, Wu D, et al. The regulation of cartilage extracellular matrix homeostasis in joint cartilage degeneration and regeneration. Biomaterials. 2021;268:120555.
22. Grogan SP, Chen X, Sovani S, Taniguchi N, Colwell CW, Lotz MK, et al. Influence of cartilage extracellular matrix molecules on cell phenotype and neocartilage formation. Tissue Eng Part A. 2014;20(1–2):264–74.
23. Chen Y, Mehmood K, Chang Y-F, Tang Z, Li Y, Zhang H. The molecular mechanisms of glycosaminoglycan biosynthesis regulating chondrogenesis and endochondral ossification. Life Sci. 2023;335:122243.
24. Rosenzweig DH, Solar-Cafaggi S, Quinn TM. Functionalization of dynamic culture surfaces with a cartilage extracellular matrix extract enhances chondrocyte phenotype against dedifferentiation. Acta Biomater. 2012;8(9):3333–41.
25. Kock L, van Donkelaar CC, Ito K. Tissue engineering of functional articular cartilage: the current status. Cell Tissue Res. 2011;347(3):613–27.
26. Lin S, Li H, Wu B, Shang J, Jiang N, Peng R, et al. TGF-β1 regulates chondrocyte proliferation and extracellular matrix synthesis via circPhf21a-Vegfa axis in osteoarthritis. Cell Commun Signal. 2022;20(1):1–18.
27. Park H, Temenoff JS, Holland TA, Tabata Y, Mikos AG. Delivery of TGF-β1 and chondrocytes via injectable, biodegradable hydrogels for cartilage tissue engineering applications. Biomaterials. 2005;26(34):7095–103.
28. Shi S, Kelly BJ, Wang C, Klingler K, Chan A, Eckert GJ, et al. Human IGF-I propeptide A promotes articular chondrocyte biosynthesis and employs glycosylation-dependent heparin binding. Biochim Biophys Acta-Gen Subj. 2018;1862(3):567–75.
29. Wen C, Xu L, Xu X, Wang D, Liang Y, Duan L. Insulin-like growth factor-1 in articular cartilage repair for osteoarthritis treatment. Arthritis Res Ther. 2021;23(1):277.
30. Liu X. BMP2 promotes chondrocyte proliferation via the Wnt/β-catenin signaling pathway. Mol Med Rep. 2011;4(4):621–6.
31. Gründer T, Gaissmaier C, Fritz J, Stoop R, Hortschansky P, Mollenhauer J, et al. Bone morphogenetic protein (BMP)-2 enhances the expression of type II collagen and aggrecan in chondrocytes embedded in alginate beads. Osteoarthritis Cartilage. 2004;12(7):559–67.
32. Lu Y, Wang Y, Zhang H, Tang Z, Cui X, Li X, et al. Solubilized cartilage ecm facilitates the recruitment and chondrogenesis of endogenous bmscs in collagen scaffolds for enhancing microfracture treatment. ACS Appl Mater Interfaces. 2021;13(21):24553–64.
33. Cao H, Wang X, Chen M, Liu Y, Cui X, Liang J, et al. Childhood cartilage ecm enhances the chondrogenesis of endogenous cells and subchondral bone repair of the unidirectional collagen–decm scaffolds in combination with microfracture. ACS Appl Mater Interfaces. 2021;13(48):57043–57.
34. Cao H, Chen M, Cui X, Liu Y, Liu Y, Deng S, et al. Cell-Free Osteoarthritis Treatment with Sustained-Release of Chondrocyte-Targeting Exosomes from Umbilical Cord-Derived Mesenchymal Stem Cells to Rejuvenate Aging Chondrocytes. ACS Nano. 2023;17(14):13358–76.

35. Pritzker KPH, Gay S, Jimenez SA, Ostergaard K, Pelletier JP, Revell PA, et al. Osteoarthritis cartilage histopathology: grading and staging. Osteoarthritis Cartilage. 2006;14(1):13–29.
36. Kawecki M, Łabuś W, Klama-Baryla A, Kitala D, Kraut M, Glik J, et al. A review of decellurization methods caused by an urgent need for quality control of cell-free extracellular matrix' scaffolds and their role in regenerative medicine. J Biomed Mater Res Part B. 2017;106(2):909–23.
37. Lei Y, Wang Y, Shen J, Cai Z, Zhao C, Chen H, et al. Injectable hydrogel microspheres with self-renewable hydration layers alleviate osteoarthritis. Sci Adv. 2022;8(5):eabl6449.

Publisher's Note